The Baseline Evaluation of LASG/IAP Climate System Ocean Model (LICOM) Version 2

LIU Hailong* (刘海龙), LIN Pengfei (林鹏飞), YU Yongqiang (俞永强), and ZHANG Xuehong (张学洪)

LASG, Institute of Atmospheric Physics, Chinese Academy of Sciences, Beijing 100029

(Received April 30, 2011; in final form Feburary 9, 2012)

ABSTRACT

The baseline performance of the latest version (version 2) of an intermediate resolution, stand-alone climate oceanic general circulation model, called LASG/IAP (State Key Laboratory of Numerical Modeling for Atmospheric Sciences and Geophysical Fluid Dynamics/Institute of Atmospheric Physics) Climate system Ocean Model (LICOM), has been evaluated against the observation by using the main metrics from Griffies et al. in 2009. In general, the errors of LICOM2 in the water properties and in the circulation are comparable with the models of Coordinated Ocean-ice Reference Experiments (COREs). Some common biases are still evident in the present version, such as the cold bias in the eastern Pacific cold tongue, the warm biases off the east coast of the basins, the weak poleward heat transport in the Atlantic, and the relatively large biases in the Arctic Ocean. A unique systematic bias occurs in LICOM2 over the Southern Ocean, compared with CORE models. It seems that this bias may be related to the sea ice process around the Antarctic continent.

Key words: LASG/IAP climate system ocean model, coordinated ocean-ice reference experiments

Citation: Liu Hailong, Lin Pengfei, Yu Yongqiang, et al., 2012: The baseline evaluation of LASG/IAP Climate system Ocean Model (LICOM) version 2. *Acta Meteor. Sinica*, **26**(3), 318–329, doi: 10.1007/s13351-012-0305-y.

1. Introduction

The first effort to develop a global ocean general circulation model (OGCM) in the State Key Laboratory of Numerical Modeling for Atmospheric Sciences and Geophysical Fluid Dynamics/Institute of Atmospheric Physics (LASG/IAP) can be traced back to the 1980s. The primary motivation for developing such an OGCM is to build a coupled atmosphere-ocean model, as well as to study the ocean circulation. Since the first 4-layer, baroclinic OGCM has been established in the later 1980s (Zhang and Liang, 1989), the family of LASG/IAP ocean models has been expanded in succession during the past 20 years. The LASG/IAP Climate system Ocean Model (LICOM; Liu et al., 2004a, b) was developed based on the third version of the LASG/IAP OGCM (Jin et al., 1999). As its previous versions, the intermediate resolution (1 degree) LICOM version 1 (LICOM1) was also the oceanic component of the LASG/IAP climate system model named Flexible Global Ocean-Atmosphere-Land System version 1 (FGOALS1) (Yu et al., 2011). FGOALS1 has participated in the Coupled Model Intercomparison Project phase 4 (CMIP4) and has been cited by the Fourth Assessment Report (AR4) of the Intergovernmental Panel on Climate Change (IPCC) (Solomon et al., 2007).

In the past several years, we aimed at reducing the uncertainties of the upper layer temperature in LICOM1, because it is crucial not only for the surface heat fluxes determining the long-term behavior of the whole climate model, but also for simulating air-sea interaction associated with climate variability on seasonal to interannual timescales. Various key physical processes in LICOM1 have been improved, including the vertical turbulent mixing scheme, the solar radiation penetration scheme (Lin et al., 2007), the advection scheme (Xiao and Yu, 2006), and the upper

Supported by the National Basic Research and Development (973) Program of China (2010CB951904 and 2007CB411806), National Natural Science Foundation of China (41075059 and 41023002), and Strategic Priority Research Program of the Chinese Academy of Sciences (XDA05110302).

*Corresponding author: lhl@lasg.iap.ac.cn.

layer taping scheme in the mesoscale eddy parameterization. Besides, the meridional resolution between 10°S and 10°N (Liu et al., 2004a) and the vertical resolution in the upper 150 m (Wu et al., 2005) are also increased to better resolve the equatorial wave-guide and the tropical thermocline, respectively. The detail of those improvements is shown in Appendix A.

Recently, all these improvements are put into version 2 of LICOM (LICOM2) and the latest version (version 2) of FGOALS (FGOALS2). The latter is taking part in the core experiments of CMIP phase 5 for the Fifth Assessment Report (AR5) of IPCC. The purpose of the present study is to document the baseline performance of the intermediate resolution (approximate 1 degree), stand-alone LICOM2 in simulating the water properties and the large-scale circulation by using metrics from Griffies et al. (2009). The evaluation aims to quantify the uncertainties of LICOM2 against the observation and to help us further understand the performance of the coupled model in the historical and projection experiments. Attempts were also made to attribute the causes of the biases in LICOM2.

The rest of the paper is organized as follows. Section 2 describes the control experiment and the observational data. Comparisons of essential metrics between LICOM2 and observation are provided in Section 3. Section 4 presents concluding remarks.

2. Control experiment and observational data

2.1 Control experiment

The Community Climate System Model (CCSM) formula and the dataset prepared by Large and Yeager (2004), which are suggested as the only forcing method and forcing dataset for the Coordinated Ocean-ice Reference Experiments (COREs; Griffies et al., 2009), are adopted in the present study. Therefore, the results from LICOM2 can be compared with the results from CORE models. In Large and Yeager formula (Large and Yeager, 2004), the surface turbulent fluxes are computed by the atmospheric state variables, including the 10-m air temperature, 10-m specific humidity, sea level pressure, 10-m wind speed, and vectors of 10-m wind. The downward solar radiation and the downward longwave radiation fluxes are both obtained from the observation. Albedo of 5.5% is used to compute the net surface shortwave radiation. The net longwave radiation is computed by the observed downward longwave radiation minus the blackbody radiation of the simulated sea surface temperature (SST). All these observational data are from the corrected Normal Year Forcing (NYF) data of COREs version 2 (Large and Yeager, 2004).

Virtual salinity flux is employed as the boundary condition for the salinity. The reference salinity is taken as 35 psu. Precipitation, evaporation, and river runoff are also from the observational dataset of Large and Yeager (2004). Besides, an extremely weak restoring term with the piston velocity of 12.5 m yr^{-1} is applied in this experiment to restore the sea surface salinity (SSS) to the observation.

Because the ocean–only model is used in the present study, observed sea ice concentration from the National Snow and Ice Data Center (NSIDC) of US over 1979–2006 is used in LICOM2. The temperature and salinity under the sea ice layer are restored to the observation from World Ocean Atlas 2005 (WOA05; Locarnini et al., 2006; Antonov et al., 2006) with a timescale of 30 days. Temperatures lower than the ice point (–1.8℃) are simply set to the ice point. To test the model sensitivity to the sea ice concentration data, an experiment using the data from the Hadley Centre of Met Office over 1948–2007 is also conducted.

The present study aims to investigate the climatological mean state of ocean in LICOM2. Therefore, following COREs phase 1, we conducted the experiment from the initial condition with WOA05 temperature and salinity and no current, forced by repeating the daily corrected NYF of Large and Yeager (2004). More details about the forcing data can be found in Table 1. LICOM2 has been integrated for 500 yr to allow the deep circulation to reach a quasi-equilibrium state. The climatology for analysis is computed over the last 10 years (491–500) of integration.

2.2 Observational data

Three datasets are used here. First, potential

Table 1. Description of the forcing data

Variable	Dataset (original)	Period	Resolution	Frequency (original)
2-m temperature	COREs v2 (NCEP/NCAR[1] reanalysis I)	1948–2007	T62	Daily (6 h)
2-m specific humidity	—	1948–2007	T62	Daily (6 h)
Surface level pressure	—	1948–2007	T62	Daily (6 h)
10-m wind	—	1948–2007	T62	Daily (6 h)
Downward shortwave radiation	COREs v2 (ISCCP[2])	1948–2007	T62	Daily (daily)
Downward longwave radiation	—	1948–2007	T62	Daily (daily)
Precipitation	COREs v2 (merging of 3 datasets[3])	1948–2007	T62	Daily (monthly)
Runoff	COREs v2	1948–2007	1°	Annual mean (annual mean)
Sea ice concentration	NSIDC	1979–2006	1°	Monthly (monthly)
SST and SSS	WOA05	Before 2005	1°	Monthly (monthly)

1 National Centers for Environmental Prediction/National Center for Atmospheric Research
2 International Satellite Cloud Climatology Project
3 Global Precipitation Climatology Project (GPCP), CPC (Climate Prediction Center) Merged Analysis of Precipitation (CMAP), and the dataset of Serrez and Hurst (2000) and Yang (1999)

temperature and salinity from WOA05 (Locarnini et al., 2006; Antonov et al., 2006) are employed to evaluate the simulated surface and sub-surface temperature and salinity. Second, meridional heat transport from Ganachaud and Wunsch (2003) is used for comparison with the simulation. Third, potential temperature and zonal current in the equatorial Pacific from Jonhson et al. (2002) are used to evaluate the results of LICOM2.

3. Results

In addition to the forcing formulation and dataset, Griffies et al. (2009) proposed a set of metrics to evaluate ocean models. Here, we pick seven primary metrics to evaluate LICOM: the horizontal averaged potential temperature and salinity, SST and SSS, the maximum mixed layer depth (MLD), the zonal averaged potential temperature and salinity, the meridional overturning stream-function, poleward heat transport (PHT), and the currents and thermocline in the tropical Pacific. Since there is no sea ice model, the sea ice variables are not included in the present study.

3.1 Horizontal averaged potential temperature and salinity

Figure 1 shows the anomalous annual mean temperature and salinity of LICOM2 as a function of depth and time against observations from WOA05. A detailed vertical structure and the evolution of the model drift are revealed. It is seen that a rapid adjustment occurs in the first 50 years. After that time, the temperature and salinity above 500 m reach a quasi-equilibrium state with cold and fresh water in the upper mixed layer and warm and fresh water in the tropical thermocline. Below 500 m, the temperature and salinity drift gradually after the first 50-yr integration, and the salinity has a slight trend even in the last 50-yr integration. This suggests that longer integration is needed to reach an equilibrium state in the deeper ocean.

The magnitudes of the model biases are about 0.6℃ and 0.2 psu for temperature and salinity, respectively. The biases are comparable with the z-coordinate model presented in Griffies et al. (2009), such as the Parallel Ocean Program (POP; about 1.5℃ and 0.2 psu) and the Modular Ocean Model (MOM; about 1℃ and 0.1 psu).

The patterns of errors in temperature and salinity from LICOM2 are different from those from the CORE models. Because the forcing formulation and dataset are similar, the errors may be caused by the difference of the model physical processes, such as the parameterization of diapycnal mixing and isopycnal mixing due to mesoscale eddy. These were also suggested by Griffies et al. (2009). The absence of the sea ice model is also a possible reason for different patterns of model drift.

3.2 SST and SSS

Figure 2a shows the SST differences between LI-

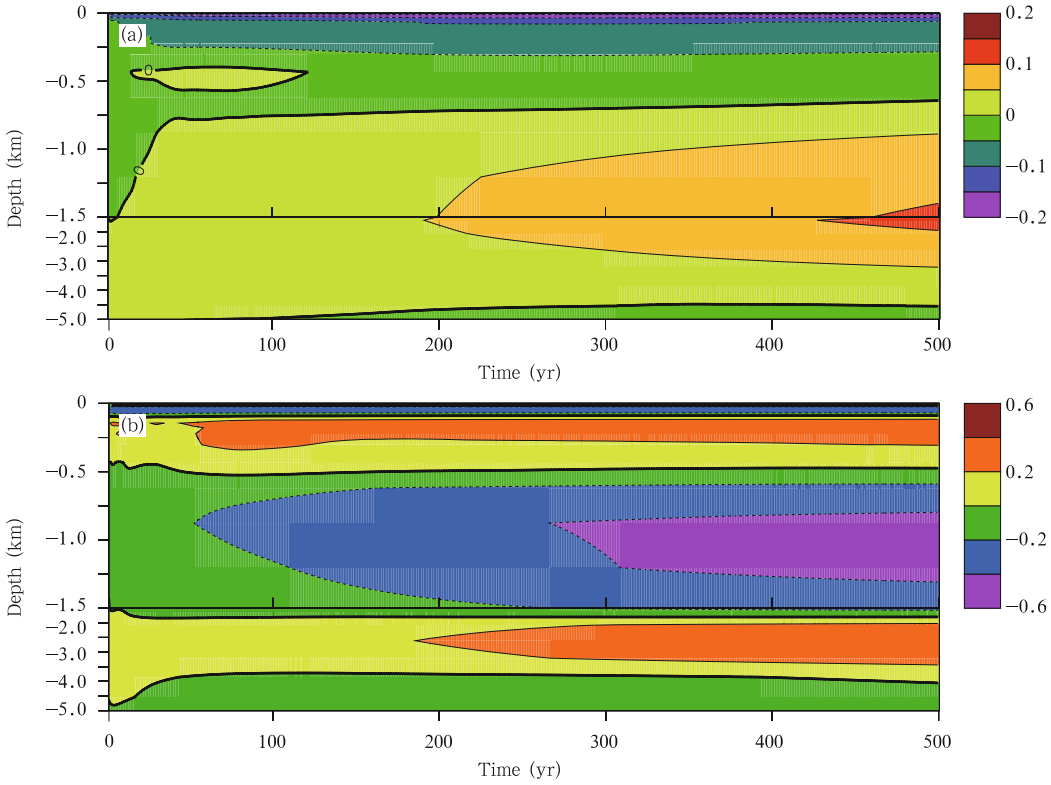

Fig. 1. Horizontal averaged drift of the annual mean (a) potential temperature (℃) and (b) salinity (psu) as a function of depth and time for LICOM2. The observation is from Locarnini et al. (2006) for (a) and Antonov et al. (2006) for (b).

COM2 and WOA05. In general, LICOM2 presents large warm biases with the area average of 0.32℃ in the tropics (20°S–20°N) and 0.64℃ in the latitudes south of 60°S. In the subtropics (20°–60°), there are slight cold biases due to the large cold and warm biases along the major fronts, such as the regions around the Kuroshio, the Gulf Stream, and the Antarctic Circumpolar Circulation (ACC), which are cancelled out with each other. The Arctic region also shows a slight warm bias.

In the tropics, there appears a large warm bias of 1℃ along the east coast of Pacific and Atlantic Ocean and a relatively small warm bias of 0.5℃ in the whole western Pacific and eastern Indian warm pool region.

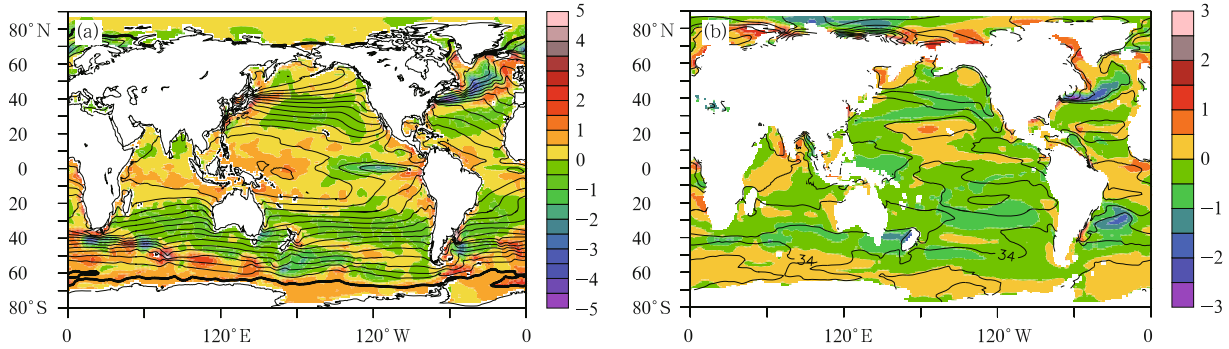

Fig. 2. (a) Sea surface temperature (℃; contour) and the difference between LICOM2 and observation from Locarnini et al. (2006) (℃; shaded), and (b) as in (a), but for sea surface salinity (psu). The observation is from Antonov et al. (2006).

The former is a common problem for the stand-alone OGCM, and it is amplified in the coupled model, the mechanism of which has been systematically investigated in some recent studies (e.g., De Szoeke and Xie, 2008; Zheng et al., 2011). Besides the large solar radiation due to the lack of low stratocumulus clouds, the weak coastal upwelling is the direct cause of the warm biases. For the OGCM, both the errors in the surface wind data and the coarse resolution may lead to the weak upwelling in this region.

Another common bias in the tropics is the exaggerated equatorial Pacific cold tongue. This is first pointed out by Stokdale et al. (1993) and is a long-lasting problem. Because the mixed layer heat budget of the cold tongue is dominated by the ocean dynamics, the errors in the vertical heat transport may be the primary cause of the cold bias. Recent studies also indicate that the lack of eddy heat transport by the tropical instability wave (TIW) can partly contribute to the spurious strong cold tongue (e.g., Jochum and Murtugudde, 2006).

In the region south of 60°S, LICOM2 exhibits a large warm bias. This is not common for the CORE models. As shown in the following subsections, the warm anomaly can be found below the surface. Therefore, the meridional density gradient, which drives ACC, is largely reduced. In the early experiments of LICOM2, the volume transport across the Drake Passage is only 81 Sv (Sv = 10^6 m^3 s^{-1}), about half of the observation of about 130 Sv (e.g., Cunningham et al., 2003). Because the surface forcing in LICOM2 is the same as the CORE models, the warm bias should be due to the internal physical processes in LICOM2.

According to previous studies (e.g., Gent et al., 2001), two sets of sensitive experiments are conducted to understand the causes of the warm bias. First, we test the sensitivity of the sea ice concentration on the warm bias. Two climatology datasets are chosen: one is from NSIDC over 1979–2006 and the other from the Hadley Centre of Met Office over 1948–2007. Figure 3 shows the annual mean difference of sea ice concentration and SST between the two experiments. Around the Antarctic, the value of Hadley Centre data is larger than that of NSIDC. This results in less surface flux released and higher warm bias in the experiment using the Hadley Centre data. Second, the sensitivity of mesoscale eddy parameterization of Gent and McWilliams (1990) on the warm bias and the magnitude of ACC has been investigated by two experiments using different isopycnal (and thickness) mixing coefficients of 500 and 1000 m^2 s^{-1}, respectively. Same as in Danabasoglu and McWilliams (1995), the smaller mixing coefficient is associated with stronger ACC and a smaller warm bias (figure omitted). This indicates that the improper mixing coefficient of the mesoscale eddy parameterization may also contribute to the warm bias in the Southern Ocean.

Except for the above two factors, the missing brine rejection process is also considered as an additional factor that causes the warm bias. This process may greatly reduce the vertical mixing and deep convection, and then weaken the overturning circulation. These are all conducive to a warm SST bias in the Southern Ocean. But further sensitive experiments are needed to investigate this process.

Figure 2b shows the SSS differences between LICOM2 and WOA05. In the present experiment, although only a weak restoring term is included in the boundary condition of salinity in the open ocean, LICOM2 simulates SSS reasonably. Except for the reg-

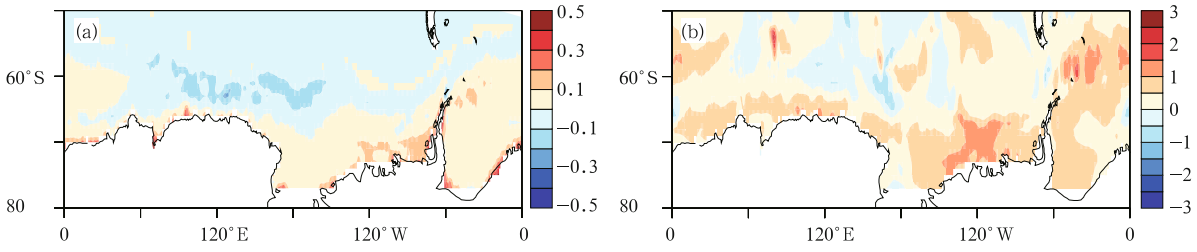

Fig. 3. The differences of (a) sea ice concentration (%) and (b) SST (℃) for two sensitive experiments using prescribed sea ice data from the Hadley Centre of Met Office and NSIDC.

ion related to the western boundary currents and near the mouth of rivers, the biases in most regions are below 0.5 psu (Fig. 2b). This magnitude is comparable with that in CORE models (Griffies et al., 2009). This indicates large uncertainties in the runoff data of CORE dataset and should be improved further.

3.3 Maximum MLD

Figure 4 shows the maximum MLD for the climatology of WOA05 and LICOM2. Following De Boyer Montégut et al. (2004), MLD here is defined as the depth of the isothermal 0.2℃ lower than the temperature at 10 m. MLD is primarily determined by the wind stirring and the static instability associated with surface buoyancy fluxes. The maximum MLD occurs during wintertime, when the surface water is cold by heat loss due to the turbulent fluxes and strong wind stirring. These processes are crucial for the water mass formation and the thermohaline circulation. Therefore, the maximum MLD is an important metrics to evaluate the ability of an ocean model to simulate these processes.

The sophisticated vertical mixing scheme and the relatively fine vertical resolution lead to a good simulation of MLD in LICOM2 in the tropics, especially in the shallow MLD region, including eastern equatorial Pacific off the western coast of Costa Rica and the southwestern equatorial India. In the region between the subtropics and subpolar gyre, MLD is much overestimated against WOA05. More heat would subduct into the tropical thermocline around 200 m. As shown in Fig. 1a, warm temperature anomaly can be found around this depth.

The discrepancies between LICOM2 and the observation can also be found in Antarctic. In LICOM2, the deep mixed layer is separated in small patches, while in observation, the distribution of the deep mixed layer is an integrated belt. As mentioned in the previous subsection, the mixing under the sea ice is supposed to be much underestimated in LICOM2 in Antarctic mainly due to the missing of the brine rejection or the largely overestimated sea ice concentration.

3.4 Zonal averaged potential temperature and salinity

Figure 5 shows the zonal averaged temperature and salinity from LICOM2 (contour) and the difference between LICOM2 and WOA05 (shaded). Because the related distribution is directly set by the global thermohaline and wind-driven circulation and is simple to obtain, this is a popular method to evaluate OGCM. Like the CORE models, the biases of LICOM2 in temperature and salinity are less than 1℃ and 0.2 psu over the most latitude-depth planes.

Comparison between Figs. 1a and 5a shows five different layers with warm biases in the tropical thermocline and around 2500 m, and cold biases at the surface, in the permanent thermocline, and at the ocean bottom. Figure 5a clearly shows the connection between the sub-surface biases and the processes at the surface: the warm anomalies in the tropical thermocline around 10° and 30°N are associated with the overestimated MLD in the North Pacific and Atlantic Ocean, the cold biases in the permanent thermocline are connected with the cold SST biases in the subtro-

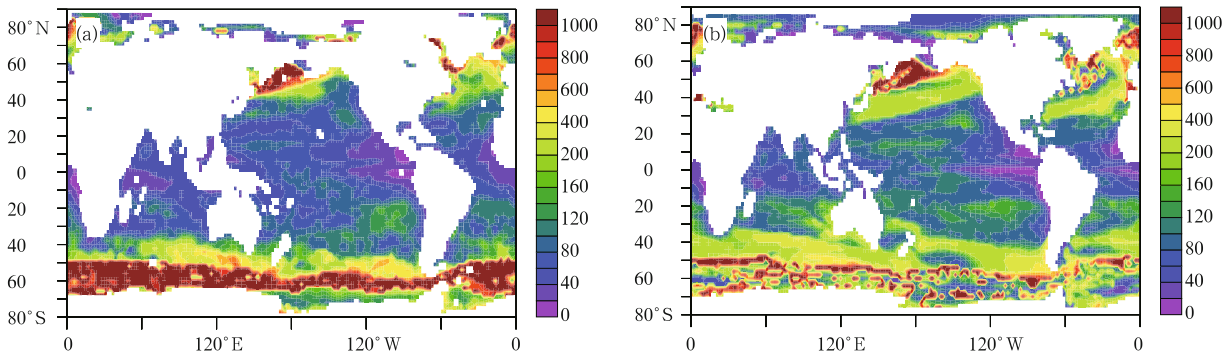

Fig. 4. The maximum mixed layer depth for the climatology of (a) WOA05 observation (Locarnini et al., 2006) and (b) LICOM2 simulation.

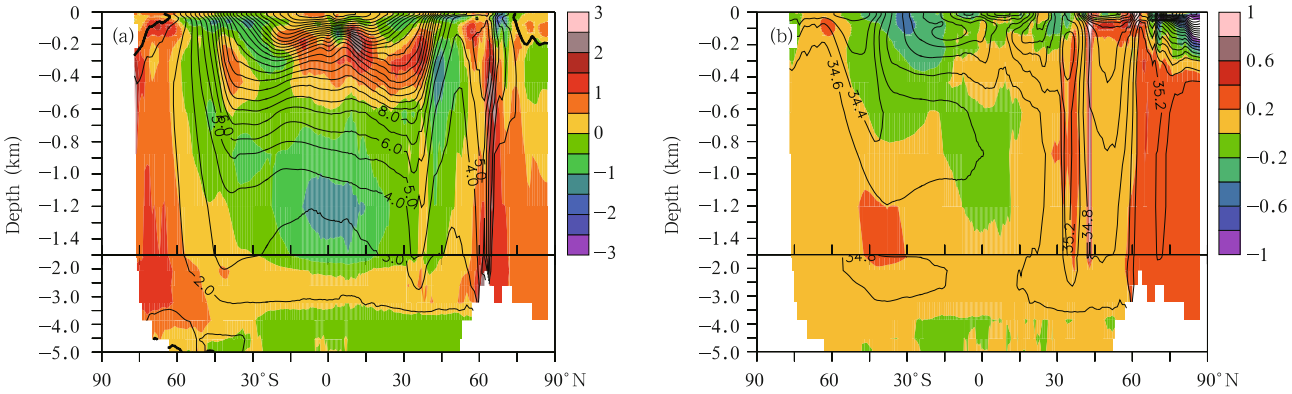

Fig. 5. (a) Zonal averaged potential temperature (℃; contour) and the difference (℃; shaded) between LIOM2 and WOA05 (Locarnini et al., 2006). (b) As in (a), but for sea surface salinity (psu). The observation is from Antonov et al. (2006).

pics, and the warm deep water around 2500 m is related to the warm biases in the polar regions. These results suggest that the surface forcing and the mixed layer processes are important for simulation of the subsurface water temperatures.

We can also find the similar relationship, but with fewer layers in the salinity field (Fig. 5b): the fresh upper layer (above 700 m), the salty main thermocline, and the fresh bottom layer. The extremely fresh bias in the upper layer can be found in the Arctic. This is associated with both runoff and sea ice processes, which have large uncertainties in the experiment. The salty bias in the thermocline also primarily occurs in the Arctic. The other two large warm biases appear around 40°S and 40°N. The former is associated with the salty water in the Southern Ocean; the latter is related to the salty water overflow from the Mediterranean (figure omitted).

We notice that the large biases in Fig. 5 mainly appear in the polar regions. Therefore, we suspect that these biases may be related to the prescribed sea ice concentration. Further experiments with LICOM2 coupled to a sea ice model forced by CORE data are undergoing to understand the mechanism of the biases.

Compared with the CORE models, the warm and salty biases around the Antarctic continent are relatively large in LICOM2, especially the warm biases. These biases reduce the meridional density gradient and weaken the transport of ACC. The volume transport through the Drake Passage is about 81 Sv in the last 10 years, which is still about 40% smaller than the observation. Besides the sea ice or mixing processes, this bias is possibly related to the entire thermohaline circulation simulation deficiency as suggested by Russell et al. (2006).

3.5 Meridional overturning stream-function

The meridional overturning stream-function is commonly used to present the features of meridional overturning circulation (MOC). Figure 6 shows the meridional overturning stream-function over the globe and in Atlantic simulated by LICOM2. LICOM2 captures the primary cells very well: the two vigorous wind-driven cells in the tropics, the Deacon Cell between 40° and 60°S, the North Atlantic Deep Water (NADW) above 3000 m north of 40°S, the bottom cell between 20° and 40°S, and the Antarctic Bottom Water (AABW) adjacent to Antarctic are all clearly shown in Fig. 6.

The volume transport of the Deacon Cell in LICOM2 is about 25 Sv, comparable with the other z-coordinate model results shown in Griffies et al. (2009). But it penetrates much deeper than that in the CORE models, and cuts off the connection between AABW and the bottom cell. This reduces the magnitude of both AABW and the bottom cell. As shown in previous subsection, the deep Deacon Cell

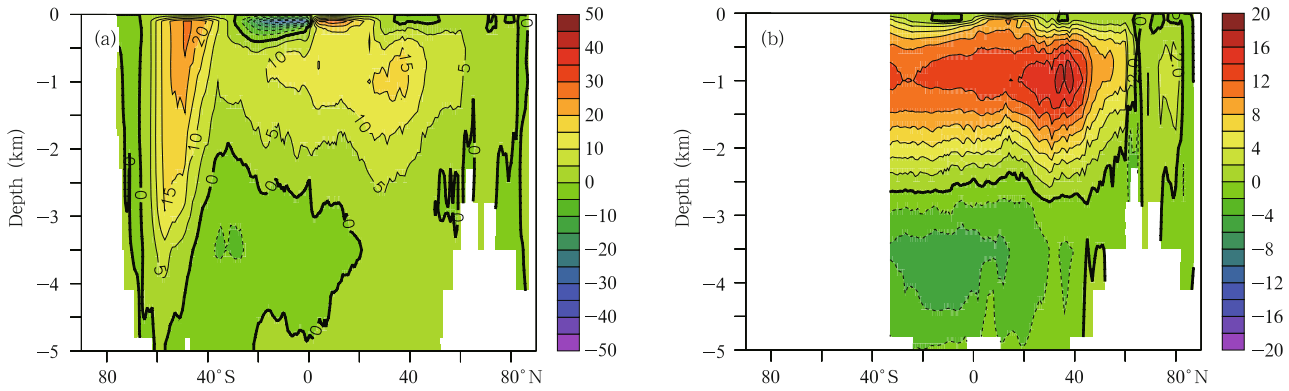

Fig. 6. (a) Global and (b) Atlantic meridional overturning stream-function (Sv = 10^6 m^3 s^{-1}) for LICOM2.

and the weak AABW may be related to the warm and salty biases around the Antarctic.

Unlike temperature and salinity, there is no directly observation of the MOC. Recently, an observing system for the MOC at 26.5°N in the Atlantic is developed under the Rapid Climate Change (RAPID) Programme of the Natural Envioronment Research Council, UK. The observed transport is 18.5 Sv averaged over 2004–2009, 4–5 Sv larger than the simulation of LICOM2 at the same latitude.

3.6 PHT

The PHT by the ocean, which is a part of the total heat transport, is primary driven by the difference of the solar heating between the tropics and the polar region. It is critical for the equilibrium of the climate system. Figure 7 shows the simulated PHT for globe and Atlantic. The dots are estimations (regarded as observations) from Ganachaud and Wunsch (2003). The total heat transport is a composite of three terms: the PHT due to the mean circulation, the PHT due to the mesoscale eddy, and the PHT due to diffusivity. The global PHT is about 1.5 PW in the Northern Hemisphere and about 1 PW in the Southern Hemisphere. These values are close to the observation. The simulation is much smaller than the observation in the Atlantic, especially between 20°S and 20°N. The weak heat transport is also the common problem for intermediate resolution OGCMs.

3.7 Thermocline and current in the equatorial Pacific

The performance of the ocean model in tropical Pacific is essential for the coupled model to simulate the interannual variability. Therefore, the thermocline and the circulation in the equatorial Pacific are also the common variables to evaluate an OGCM. Figure 8 shows the temperature along equatorial Pacific for the observation from Jonhson et al. (2002) and for LICOM2. The warm bias in the warm pool and cold

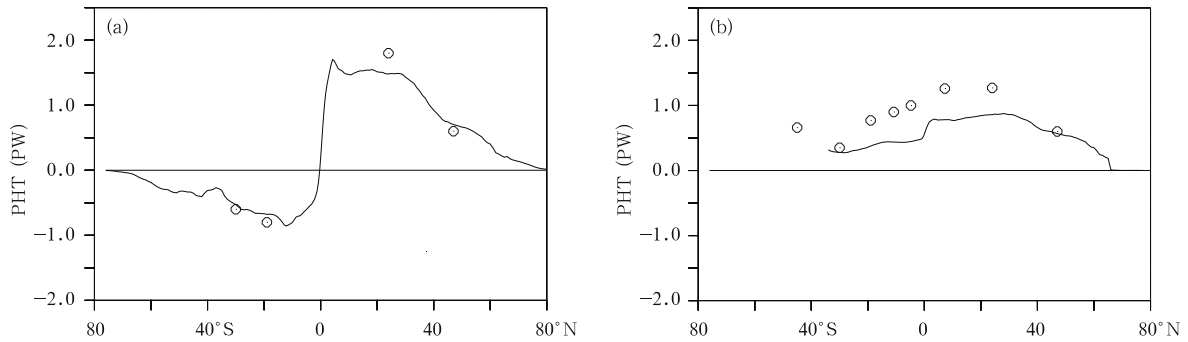

Fig. 7. (a) Global and (b) Atlantic polarward heat transport (PHT; PW = 10^{15} W) for LICOM2 (solid). The dots are estimations from Ganachaud and Wunsch (2003).

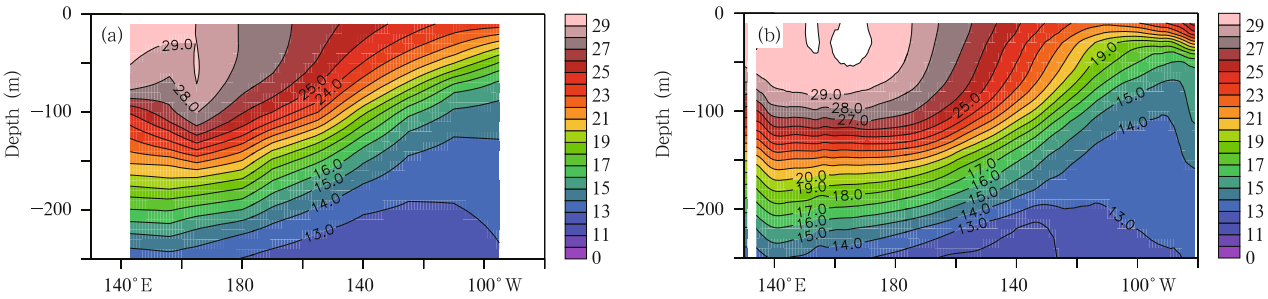

Fig. 8. The potential temperature (℃) along the equatorial Pacific for (a) Jonhson et al. (2002) and (b) LICOM2.

bias in the cold tongue, which are mentioned in subsection 3.2, are also clearly seen in Fig. 8. The rise of the tropical thermocline in the eastern Pacific indicates that the strong equatorial upwelling causes the cold bias. The tropical thermocline in LICOM2 is more compact than in the previous version (figure omitted).

Figure 9 shows the zonal current along the equatorial Pacific for the observation from Jonhson et al. (2002) and for LICOM2. Through reducing horizontal viscosity from 2×10^4 to 3×10^3 m^2 s^{-1}, the simulated pattern of zonal current along the equator is significantly improved. Therefore, the Equatorial Under Current (EUC) in the thermocline is increased to 0.7 m s^{-1}. Although the EUC is about 30% less than that of observation, this is still a reasonable value for an intermediate resolution OGCM.

4. Concluding remarks

In the present study, the baseline performance of the intermediate resolution, stand-alone OGCM, LICOM2, has been evaluated against the observation by using main metrics from Griffies et al. (2009). In general, the errors in the water properties and in the circulation are comparable with the CORE models. Some common problems of OGCM also appear in LICOM2, such as the cold bias in the eastern Pacific cold tongue, the warm biases off the eastern coast of the basins, the weak poleward heat transport in the Atlantic, and the relatively large biases in the Arctic Ocean. A unique systematic bias occurs in LICOM2 over the Southern Ocean compared with CORE models. The biases can be found in both the stratification and the circulation, such as the warm and salty biases around 2500 m, the weak transport of ACC and the deep penetration of Deacon Cell. It seems that this bias may be related to the sea ice process around the Antarctic.

A systematic comparison between LICOM1 and LICOM2 is undergoing. Preliminary results indicate that the performance of LICOM2 has been substantially improved in many aspects, mainly including the shallow MLD in the eastern Pacific and western India, the small temperature and salinity biases in the depth-latitude plane, the increasing MOC in the Atlantic, the increasing EUC, etc. The updated vertical mixing scheme, the increase of vertical resolution, and the reduction of the viscosity are all considered to have contributed to these improvements. But more sensi-

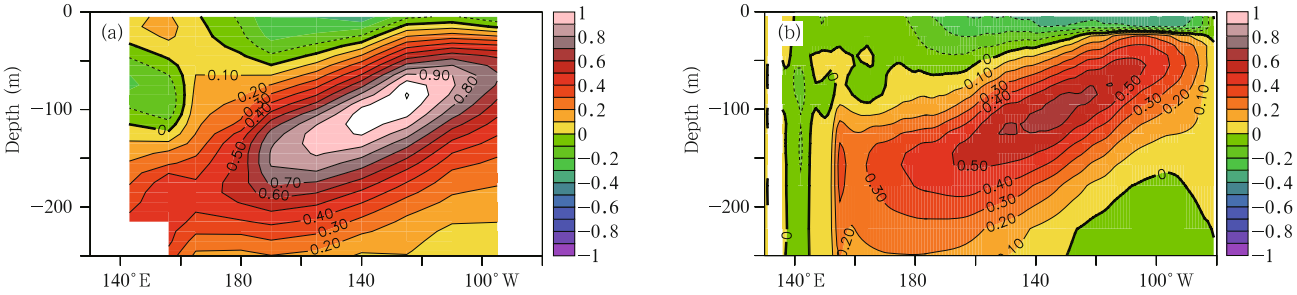

Fig. 9. The zonal current (m s^{-1}) along the equatorial Pacific for (a) Jonhson et al. (2002) and (b) LICOM2.

tive experiments are needed to further identify the effect of each process.

In this study, the performance of LICOM2 has been investigated by using an equilibrium simulation. To understand the model behavior, the ability of the model in simulating the climatic variability on intraseasonal to intradecadal timescales also needs to be further evaluated. This work is also undergoing.

The model used in the current study is an ocean-only model, rather than an ocean-ice coupled model as that of the CORE models. The results of this work are therefore not good for comparison with the results of CORE models, especially in the high latitudes and for deep circulations. Because the process related to the sea ice can affect not only the local temperature and salinity, but also the remote region through modifying the thermohaline circulation. Thus, the ocean-sea ice coupled experiment is also needed.

Acknowledgments. We thank the two anonymous reviewers for their helpful comments and suggestions that have improved the manuscript.

Appendix A. Brief description of improvements of LICOM2 from LICOM1

The fundamental framework of LICOM2 is inherited from LICOM1. The primary features include the η-coordinate, free surface, primitive equation, and mesoscale eddy parameterization from Gent and McWilliams (1990), etc. The main improvements of LICOM2 are listed in Table A1.

Table A1. Main improvements of LICOM2 from LICOM1

	LICOM1	LICOM2
Horizontal resolution	1°×1°	1°×(0.5°–1°)
Vertical resolution	30 levels (25 m in the upper 300 m)	30 levels (10 m in the upper 150 m)
Advection scheme	2-order central difference	A shape-preserving (Yu, 1994)
Vertical mixing	Pacanowski and Philander (1981)	Canuto et al. (2001, 2002)
Mesoscale eddy parameterization	Gent and McWilliams (1990), 1000 m^2 s^{-1}	Gent and McWilliams (1990), 500 m^2 s^{-1}; Large et al. (1997)
Horizontal viscosity	2×10^4 m^2 s^{-1}	3×10^3 m^2 s^{-1}
SW radiation penetration	Constant (Paulson and Simpson, 1977)	Chlorophyll dependent (Ohlmann, 2003)
Forcing formula and dataset	Restoring; Max-Planck-Institute Ocean Model Intercomparison Project forcing and World Ocean Atlas 98	Large and Yeager (2004); COREs

A.1 Resolution

Because of the smaller length scale, which is always measured by the first baroclinic Rossby radius of deformation, in the ocean than that in the atmosphere, the horizontal resolution is crucial for ocean circulation simulation. To better resolve the equatorial wave-guide with an acceptable computational cost, the meridional resolution between 10°S and 10°N has been increased from 1° to 0.5°. The grid distance between 10° and 20° gradually varies from 0.5° to 1°.

To improve the simulation of the upper ocean, the vertical level of LICOM has been rearranged following Wu et al. (2005). The number of levels in the upper 150 m has been more than doubled, increasing from 6 to 15 levels.

A.2 Physical processes

Besides the resolution, the physical parameterization schemes have also been improved in LICOM2. First, the scheme dependent on Richardson number (Pacanowski and Philander, 1981; called PP scheme hereafter) for vertical turbulence mixing was replaced by a second-order turbulence closure model of Canuto et al. (2001, 2002; called Canuto scheme hereafter). The PP scheme intends to describe the mixing in the tropical thermocline where the mixing is mainly due to large velocity shear close to EUC. Therefore, the PP scheme is only valid in the tropics, usually from

30°S to 30°N. The Canuto scheme is valid globally; it includes not only the mixing due to the velocity shear but also the mixing due to the internal-wave break and double diffusion. After using the Canuto scheme, the discontinuity of water properties between the tropics and extra-tropics has been eliminated since the same vertical mixing scheme is applied over the entire model domain. Thus, the horizontal viscosity can be reduced from 2×10^4 to 3×10^3 m^2 s^{-1}.

Second, we have modified the mesoscale eddy parameterization of Gent and McWilliams (1990; called GM90 hereafter), which is usually used to replace the horizontal mixing and to correct the spurious diapycnal mixing in the z-coordinate ocean model. The scheme in LICOM1 is adopted from MOM version 2 (Jin et al., 1999) with the isopycnal mixing and thickness mixing coefficients both assigned to 1000 m^2 s^{-1}, and the maximum slope of isophycnals set to 0.01. To reduce the mesoscale mixing in the upper layer, the isopycnal and thickness diffusivities have been tapered by the method of Large et al. (1997). Additionally, in order to simulate a stronger Antarctic Circumpolar Circulation (ACC), the isopycnal and thickness mixing coefficients are reduced from 1000 to 500 m^2 s^{-1} following Danabasoglu and McWilliams (1995).

Third, the two-exponent scheme with constant coefficients of Paulson and Simpson (1977; called PS77 hereafter), has been substituted by a scheme of Ohlmann (2003), in which all the parameters are functions of chlorophyll concentration. Lin et al. (2007) compared the differences of SST between the two schemes in the eastern equatorial Pacific.

In addition, a shape-preserving advection scheme of Yu (1994) was incorporated into LICOM2 by Xiao and Yu (2006). The excessive equatorial cold tongue has been significantly reduced due to the improvement of the advection scheme. Therefore, in the present study, we still use the Yu (1994) scheme in the experiment.

A.3 Other improvements

There are also improvements in computing techniques and fixing of bugs in LICOM2. These improvements or corrections are vital for the accuracy and efficiency of the model. The improvements primarily include the following: changing the computation of arrays and variables from single precision to double precision; optimizing the parallel performance; correcting bugs in the restart process, etc. A two-dimensional partition version of LICOM has also been developed, but only for the eddy-resolving version of LICOM2 by far.

REFERENCES

Antonov, J. I., R. A. Locarnini, T. P. Boyer, et al., 2006: *World Ocean Atlas 2005, Volume 2: Salinity.* NOAA Atlas NESDIS 62, US, Washington D. C., 1–182.

Canuto, V. M., A. Howard, Y. Cheng, et al., 2001: Ocean turbulence. Part I: One-point closure model-momentum and heat vertical diffusivities. *J. Phys. Oceanogr.*, **31**, 1413–1426.

——, ——, ——, et al., 2002: Ocean turbulence. Part II: Vertical diffusivities of momentum, heat, salt, mass, and passive scalars. *J. Phys. Oceanogr.*, **32**, 240–264.

Cunningham, S., S. Alderson, B. King, et al., 2003: Transport and variability of the Antarctic Circumpolar Current in Drake Passage. *J. Geophys. Res.*, **108**, 8084–8100.

Danabasoglu, G., and J. McWilliams, 1995: Sensitivity of the global ocean circulation to parameterizations of mesoscale tracer transports. *J. Climate*, **8**, 2967–2987.

De Boyer Montégut, C., G. Madec, A. S. Fischer, et al., 2004: Mixed layer depth over the global ocean: an examination of profile data and a profile-based climatology. *J. Geophys. Res.*, **109**, C12003, doi: 10.1029/2004JC002378.

De Szoeke, S. P., and Shangping Xie, 2008: The tropical eastern Pacific seasonal cycle: Assessment of errors and mechanisms in IPCC AR4 coupled ocean-atmosphere general circulation models. *J. Climate*, **21**, 2573–2598.

Ganachaud, A., and C. Wunsch, 2003: Large-scale ocean heat and freshwater transports during the world ocean circulation experiment. *J. Climate*, **16**, 696–705.

Gent, P., and J. C. Mcwilliams, 1990: Isopycnal mixing in ocean circulation models. *J. Phys. Oceanogr.*, **20**, 150–155.

Gent, P. R., W. G. Large, and F. O. Bryan, 2001: What sets the mean transport through Drake Passage? *J.*

Geophys. Res., **106**, 2693–2712.

Griffies, S., and Coauthors, 2009: Coordinated ocean-ice reference experiments (COREs). *Ocean Modelling*, **26**, 1–46.

Jin Xiangzhe, Zhang Xuehong, and Zhou Tianjun, 1999: Fundamental framework and experiments of the third generation of IAP/LASG world ocean general circulation model. *Adv. Atmos. Sci.*, **16**, 197–215.

Jochum, M., and R. Murtugudde, 2006: Temperature advection by tropical instability waves. *J. Phys. Oceanogr.*, **36**, 592–605.

Johnson, G. C., B. M. Sloyan, W. S. Kessler, et al., 2002: Direct measurements of upper ocean currents and water properties across the tropical Pacific Ocean during the 1990s. *Prog. Oceanogr.*, **52**, 31–61.

Large, W., G. Danabasoglu, S. Doney, et al., 1997: Sensitivity to surface forcing and boundary layer mixing in a global ocean model: Annual-mean climatology. *J. Phys. Oceanogr.*, **27**, 2418–2447.

——, and S. Yeager, 2004: Diurnal to Decadal Global Forcing for Ocean and Sea-Ice Models: The Data Sets and Flux Climatologies. NCAR/TN-460+STR, 1–105.

Lin Pengfei, Liu Hailong, and Zhang Xuehong, 2007: Sensitivity of the upper ocean temperature and circulation in the equatorial Pacific to solar radiation penetration due to phytoplankton. *Adv. Atmos. Sci.*, **24**, 765–780.

Liu Hailong, Zhang Xuehong, Li Wei, et al., 2004a: A eddy-permitting oceanic general circulation model and its preliminary evaluations. *Adv. Atmos. Sci.*, **21**, 675–690.

——, Yu Yongqiang, Li Wei, et al., 2004b: *Manual for LASG/IAP Climate System Ocean Model (LICOM1.0)*. Science Press, Beijing, 128 pp. (in Chinese)

Locarnini, R. A., A. V. Mishonov, J. I. Antonov, et al., 2006: *World Ocean Atlas 2005, Volume 1: Temperature*. NOAA Atlas NESDIS 61, US, Washington D. C., 1–182.

Ohlmann, J., 2003: Ocean radiant heating in climate models. *J. Climate*, **16**, 1337–1351.

Pacanowski, R., and S. Philander, 1981: Parameterization of vertical mixing in numerical models of tropical oceans. *J. Phys. Oceanogr.*, **11**, 1443–1451.

Paulson, C., and J. Simpson, 1977: Irradiance measurements in the upper ocean. *J. Phys. Oceanogr.*, **7**, 952–956.

Russell, J. L., R. J. Stouffer, and K. W. Dixon, 2006: Intercomparison of the Southern Ocean circulations in IPCC coupled model control simulations. *J. Climate*, **19**, 4560–4575.

Serrez, M., and C. Hurst, 2000: Representation of mean Arctic precipitation from NCARP/NCAR and ERA reanalyses. *J. Climate*, **13**, 182–201.

Solomon, S., D. Qin, M. Manning, et al., 2007: *Climate Change 2007: The Physical Science Basis*. Cambridge University Press, Cambridge, United Kingdom and New York, NY, USA, 996 pp.

Stockdale, T., and Coauthors, 1993: Intercomparison of tropical ocean GCMs. World Circulation Programme Research Memo, WCRP-79, 1–67.

Wu Fanghua, Liu Hailong, Li Wei, et al., 2005: Effect of adjusting vertical resolution on the eastern equatorial Pacific cold tongue. *Acta Meteor. Sinica*, **24**, 1–12.

Xiao Chan and Yu Yongqiang, 2006: Adoption of a two-step shape-preserving advection scheme in an OGCM. *Progress in Natural Science*, **16**, 1442–1448.

Yang, D., 1999: An improved precipitation climatology for the Arctic Ocean. *Geophys. Res. Lett.*, **26**, 1625–1628.

Yu Rucong, 1994: A two-step shape-preserving advection scheme. *Adv. Atmos. Sci.*, **11**, 479–490.

Yu Yongqiang, Zheng Weipeng, Wang Bin, et al., 2011: Versions g1.0 and g1.1 of the LASG/IAP Flexible Global Ocean-Atmosphere-Land System Model. *Adv. Atmos. Sci.*, **28**, 99–117.

Zhang Xuehong and Liang Xinzhong, 1989: A numerical world ocean general circulation model. *Adv. Atmos. Sci.*, **6**, 43–61.

Zheng, Y., T. Shinoda, J. L. Lin, et al., 2011: Sea surface temperature biases under the stratus cloud deck in the Southeast Pacific Ocean in 19 IPCC AR4 coupled general circulation models. *J. Climate*, **24**, 4139–4164.